

Cross-Field-Current Driven Lower-Hybrid Instability and Stochastic Ion Heating*

M. Yamada and D. K. Owens

Plasma Physics Laboratory, Princeton University, Princeton, New Jersey 08540

(Received 14 March 1977)

A suprathermal electron beam is injected parallel to \vec{B} in a low- β plasma. The sharp space-potential drop across the surface of the beam generates a strong cross-field current which in turn drives a modified two-stream instability at the lower hybrid frequency. Intense stochastic ion heating is observed with the onset of the instability, and the heating rate is found to be proportional to the wave energy.

Heating a plasma by injecting high-energy charged or neutral-particle beams is a topic of major interest in fusion plasma physics. We have investigated a fundamental process in the interaction between an injected high-energy electron beam and a target plasma.

In past years, cross-field-current driven microinstabilities have been intensively studied,^{1,2} particularly in connection with anomalous ion heating in plasmas produced by relativistic electron beam injection into mirror machines,³ θ pinches,⁴ and collisionless shock experiments.⁴ Among these instabilities, a low-hybrid instability, with frequency between the electron and ion cyclotron frequencies ($\omega_{ci} < \omega_{LH} < \omega_{ce}$), is easily destabilized by $\vec{E} \times \vec{B}$ current. This instability often occurs as a flute-type nonresonant mode and can play an important role in enhanced ion heating.⁵ In contrast to ion acoustic waves, lower-hybrid waves are not subject to strong ion Landau damping even in isothermal ($T_e \approx T_i$) plasmas and can have a large growth rate ($\gamma \sim \omega$).

In this Letter, we report a new experimental identification of the modified two-stream lower-hybrid instability and the resultant stochastic ion heating in a laboratory plasma, not only in steady state but also in pulsed operation. A significant result of the present experiment is the first detailed study of the relation between the excited wave amplitude and the ion heating rate (time resolution: $t < 2 \mu\text{sec}$), elucidating the stochastic ion heating which is due to the lower-hybrid instability.

The experiments were performed on the thermally ionized potassium plasma of the Princeton Q-1 device,⁶ Fig. 1(a). The plasma column (diameter 3.2 cm, confining field 2–6 kG, $T_{e0} \approx T_{i0} = 0.35 \text{ eV}$, and $n_{e0} \approx 10^9 \text{ cm}^{-3}$) is divided by a negatively biased mesh (grid spacing $< \lambda_D$). If the beam-source end plate is biased at a potential somewhat higher than the mesh voltage and the target-plasma end plate is grounded, electrons

flow through the mesh with more than thermal velocity into the target plasma; high electron conductivity lowers the potential in the beam region. The beam, well defined by a mechanical aperture ($r = 2 \sim 4 \text{ mm}$), has a velocity $v_b \approx (2eV_{\text{bias}}/m)^{1/2}$ and density $n_b \propto n_0 \exp[(V_{\text{bias}} - V_{\text{mesh}})/T]$. The important feature is that the sharp drop in plasma potential at the radial surface of the electron beam, creates a strong cross-field azimuthal electron current [$c(\vec{E} \times \vec{B})/B$] at the surface, Fig. 1(b). Ion $\vec{E} \times \vec{B}$ motion is negligible because of the high ion inertia and $(1/\varphi)(d\varphi/dr) \gg 1/\rho_i$. Collisional effects are negligible.

With the injection of a low-density beam ($n_{eb}/n_{e0} \ll 1$, $eV_b \gg kT_e$) we observe the familiar electron-electron two-stream instability which has

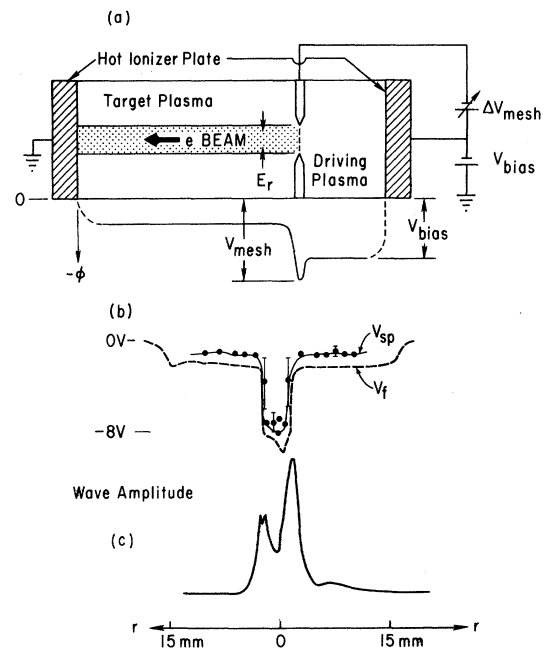


FIG. 1. (a) Schematic diagram of setup; (b) radial space (V_{sp}) and floating (V_f) potential profiles; (c) wave amplitude profile.

been well investigated.⁷ The peak frequency is somewhat below the electron plasma frequency, and neither fluctuations below the ion plasma frequency nor ion heating are detected in this condition.

On the other hand, with a high-density beam ($n_{eb}/n_{e0} \lesssim 1$), we observe a new instability ($\omega \simeq \omega_{LH} \simeq \omega_{pi}$) destabilized at the periphery of the injected beam. The identification of this instability and the resultant ion heating are the subject of this Letter. Figure 1(b) depicts the potential profile. The radial space-potential profile agrees with the floating-potential profile since most of the electrons in the beam region are supplied through the mesh and charge neutrality is maintained by the reduction of the electron supply from the target end plate. Figure 1(c) presents the measured wave amplitude versus radial position. The amplitude of the instability peaks at a few cyclotron harmonics clustered near the lower-hybrid frequency, Fig. 2(a), and the center of the spectrum shifts with the target plasma density. Propagation is predominantly azimuthal [in the slab model, $k_y > k_x \gg k_z \simeq \pi/2L$; L is the machine length (10^2 cm)] in the direction of the $\vec{E} \times \vec{B}$ drift. Figure 2(b) presents the azimuthal phase velocity versus magnetic field strength B , showing $\omega/k_y \sim B^{-0.7}$. Since the parallel wavelength, λ_z , is longer than the machine length, there is no parallel resonance effect⁸ between the injected beam velocity and the wave propagation. The observations are in agreement with numerical calculations of the modified two-stream instability.¹

Theoretically, we consider a low- β Maxwellian target plasma in a straight magnetic field $B\hat{z}$ with

$$1 - \frac{k_z^2}{k^2} \frac{\omega_{pe}^2}{(\omega - \vec{k} \cdot \vec{u})^2} + \frac{k_{Di}^2}{k^2} \left\{ 1 + \sum_{n=-\infty}^{\infty} I_n(\lambda) e^{-\lambda} \frac{\omega}{k_z v_i} Z \left(\frac{\omega - n\omega_{ci}}{k_z v_i} \right) \right\} = 0, \quad (1)$$

where $\lambda = k^2 \rho_i^2 / 2$, $\rho_i = (2T_i / M\omega_{ci}^2)^{1/2}$, $v_i = (2T_i / M)^{1/2}$, I_n is the modified Bessel function of n th order, and Z is the plasma dispersion function with conventional definitions.¹ We have neglected the electron diamagnetic drift since probe measurements indicate that the electron density gradient is small at the beam surface.⁹ We have also assumed that all electrons are drifting with the macroscopic azimuthal velocity at the beam surface.

In the present experiment, with $10^{-2} < (k_z^2/k^2) \times (M/m) \lesssim 1$ and $\omega_{pi}/\omega_{ci} \simeq 3 \sim 10$, a numerical calculation of Eq. (1) predicts the most unstable modes somewhat below ω_{pi} , with a few cyclotron

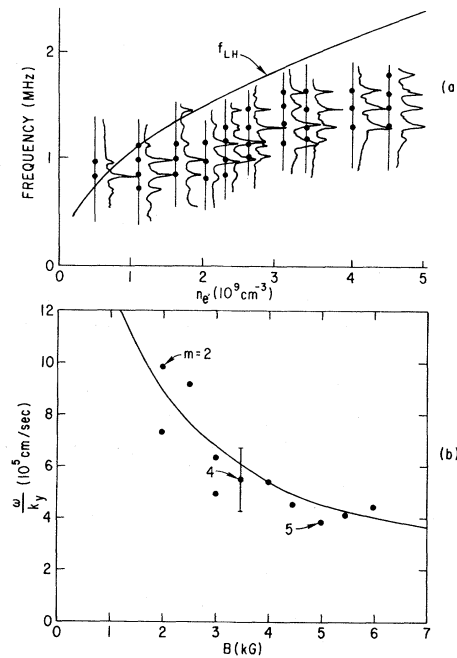


FIG. 2. (a) Frequency spectrum vs target plasma density. Solid curve denotes $f_{LH} \simeq f_{pi}$, $B = 4$ kG. (b) Azimuthal phase velocity vs B . Solid line is calculation in the fluid limit calibrated at $B = 5.5$ kG, for fixed $k_z = \pi/2L$, $eV_{bias} = 8$ eV. $u_{E \times B} \simeq (6 \pm 3) \times 10^5$ cm/sec for 5.5 kG; m denotes azimuthal mode number.

$T_e = T_i = T_0$ and an electron beam with streaming velocity $u = u_{\parallel} \hat{z} + u_{\perp} \hat{y}$ and temperature $T_e \simeq T_0$. The dispersion relation for electrostatic waves propagating nearly perpendicular to \vec{B} ($k_{\perp} \gg k_z$ and $\omega/k_z v_e > 1$), for $k_{\perp} \rho_e \ll 1 \lesssim k_{\perp} \rho_i$ and $\omega_{pe} \ll \omega_{ce}$, is written at the beam surface:

harmonics.^{1,10} The phase velocity of the wave is close to the $\vec{E} \times \vec{B}$ drift velocity of the electrons at the beam surface. These features are compared with the experiment in Fig. 2.

In order to investigate in detail the relation between the wave amplitude and ion heating, a pulsed electron beam ($\tau_{rise} \lesssim 1 \mu\text{sec}$) is injected. The absolute value of the wave amplitude is measured with a probe calibrated by comparing dc and rf probe detection characteristics. The very large saturated amplitude ($e\tilde{\phi}/T_{e0} \sim 1$) invokes modification of ion orbits in the wave potential trough.¹ However, in the present open-system

experiment the wave saturation is considered to be due to modification of the electron's velocity and space distribution at the beam edge. Parallel and perpendicular ion temperatures are measured using a small Faraday cup (size 2 mm, located outside of the electron beam) in which the separation between the electron shielding grid and collector is less than 0.2 mm. The collector current signal is analyzed with boxcar sampling at a resolution time shorter than 2 μ sec. In all cases, the wave amplitude saturates within a few microseconds ($\tau_{\text{growth}} \sim 3/\omega_{pi} \lesssim \tau_{\text{rise}}$), after which strong ion heating occurs, Fig. 3. The deviation from the computer simulation results¹ in which T_i increases with wave amplitude is considered to be

$$\frac{dT_{i\perp}}{dt} \simeq \omega_{pi}^2 \left\{ \sum_k \frac{\langle |\tilde{E}_k|^2 \rangle}{4\pi n_0} \left[\frac{\nu_c(k)}{\omega^2} + (4\pi)^{1/2} \frac{\omega^2}{k^3 v_i^3} \exp\left(-\frac{\omega^2}{k^2 v_i^2}\right) \right] \right\}. \quad (2)$$

Usually a quasilinear theory (QLT) is used for weakly turbulent plasma or in the linear growth state in which $\Delta\omega_{\text{spectrum}} > \gamma$, $\Delta(\omega/k) > v_{\text{trap}}$. This instability with large growth rate quickly reaches a highly nonlinear stationary turbulent state, apparently not relevant to QLT. However, if one renormalizes QLT by introducing stochasticity as $\nu_c(k)/k \simeq \Delta(\omega/k) > v_{\text{trap}}$ ($\nu_c < \omega$), the theory can again be used to estimate energy transfer from waves to ions. The second term represents reso-

nant ion heating ($\omega \gg \omega_{ci}$) and is much smaller than the first for the present conditions. An estimate of $\nu_c \simeq \omega_{ci} \simeq \text{const.} \lesssim \gamma$ is supported by the observed constant spectrum width, $\Delta\omega$, and the correlation of the signals from two probes

According to renormalized quasilinear theory,¹¹ the ion heating rate can be expressed as

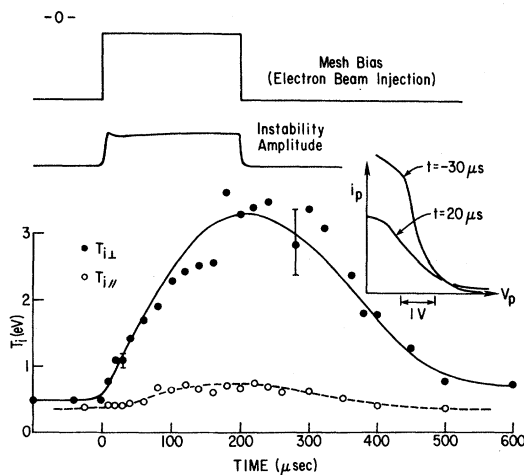


FIG. 3. Pulsed operation. From top, mesh bias, instability amplitude, and perpendicular (closed circles, $T_{i\perp}$) and parallel (open circles, $T_{i\parallel}$) ion temperatures are plotted vs time. $B = 4$ kG. Typical ion-current I - V curves of the energy analyzer are also shown in the corner. The decrease of the saturation current is mostly due to the density reduction caused by the instability.

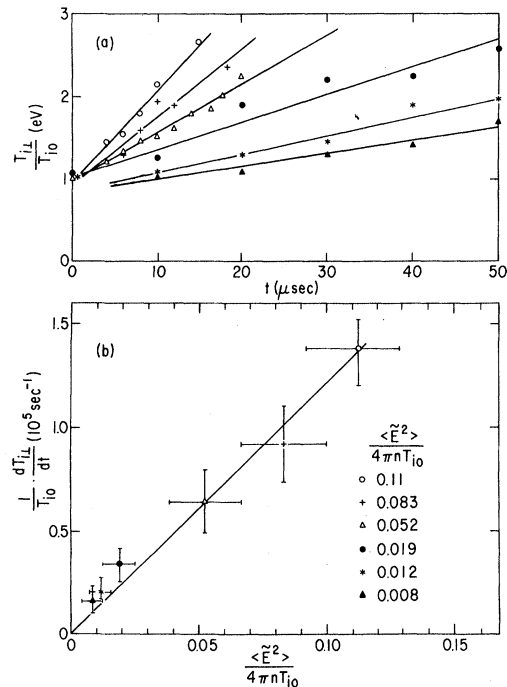


FIG. 4. (a) $T_{i\perp}$ vs time for various $\vec{E} \times \vec{B}$ pumping energies. Waves saturate within a few microseconds. (b) Ion heating rate vs the instability energy. $B = 4$ kG, $n_{e0} = 1.2 \times 10^9 \text{ cm}^{-3}$.

separated by $y = 2\pi/k_{\perp}$.^{12,13} Substituting the measured values of $\nu_c(k) \approx 0.1\omega_{pi}$, $\sum_k \tilde{E}_k^2/4\pi n_0 T_{i0} \approx 0.04$, $\omega_{\text{peak}} \approx \frac{2}{3}\omega_{pi}$, we obtain $(1/T_{i0})(dT/dt) = 0.009\omega_{pi}$, corresponding to $\tau_{\text{heating}} \approx 20 \mu\text{sec}$, in agreement with Fig. 3.

To check the quasilinear heating rate, Fig. 4(a) presents the $T_{i\perp}$ increase versus time for various saturated wave energies. As seen in Fig. 4(b), the ion-heating rate is proportional to the saturated wave energy, quantitatively confirming the quasilinear relation with $\nu_c \approx \text{constant}$. Furthermore, since we have observed a linear relation between the saturated wave energy and the radial voltage drop (pumping energy), the ion heating rate is proportional to the power input through the $\vec{E} \times \vec{B}$ motion of the electrons. A similar result is obtained for the electron heating rate in parametrically driven instabilities.¹⁴

It is a pleasure to thank Dr. R. Z. Sagdeev, Dr. T. H. Stix, Dr. V. Arunasalam, Dr. H. W. Hendel, Dr. H. Ikezi, and Dr. P. Kaw for valuable discussions and suggestions, and S. Seiler for his help with the ion-probe instrumentation.

*Work supported by U. S. Energy Research and Development Administration Contract No. E(11-1)-3073.

¹John B. McBride *et al.*, Phys. Fluids 15, 2367 (1972); Edward Ott *et al.*, Phys. Rev. Lett. 28, 88 (1972); Nicholas A. Krall and Paulett C. Liewer, Phys. Rev. A 4, 2094 (1971); C. N. Lashmore-Davies and T. J. Martin,

Nucl. Fusion 13, 193 (1973); P. J. Barrett *et al.*, Phys. Rev. Lett. 28, 337 (1972).

²Y. Kitagawa *et al.*, J. Phys. Soc. Jpn. 41, 1041 (1976).

³I. Alexeff *et al.*, Phys. Rev. Lett. 25, 848 (1970), and in *Proceedings of the Fourth International Conference on Plasma Physics and Controlled Nuclear Fusion Research, Madison, Wisconsin, 1971* (International Atomic Energy Agency, Vienna, Austria, 1972).

⁴M. Keilhacker and K. H. Steur, Phys. Rev. Lett. 26, 694 (1971); R. J. Commisso and H. R. Griem, Phys. Rev. Lett. 36, 1038 (1976).

⁵R. C. Davidson and N. T. Gladd, Phys. Fluids 18, 1327 (1975).

⁶R. J. Taylor *et al.*, Rev. Sci. Instrum. 43, 1675 (1972).

⁷R. J. Briggs, *Electron-Stream Interaction with Plasmas* (MIT Press, Cambridge, Mass., 1964); J. H. Malmberg and C. B. Wharton, Phys. Fluids 12, 2600 (1969).

⁸K. Papadopoulos and P. Palmadesso, Phys. Fluids 19, 605 (1976).

⁹This condition satisfies the opposite inequality of Eq. (3) of Ref. 2.

¹⁰D. W. Forslund *et al.*, Phys. Rev. Lett. 25, 1266 (1970).

¹¹I. Ichimaru, J. Phys. Soc. Jpn. 39, 1373 (1975); A. Hirose and I. Alexeff, Phys. Rev. Lett. 28, 1176 (1972).

¹²G. R. Smith and A. N. Kaufman, Phys. Rev. Lett. 34, 1613 (1975).

¹³A. Fukuyama *et al.*, Institute for Plasma Physics, Nagoya University, Report No. IPPPJ-259, 1976 (unpublished).

¹⁴M. Porkolab *et al.*, Nucl. Fusion 16, 269 (1976); H. W. Hendel and J. T. Flick, Phys. Rev. Lett. 31, 199 (1973).

Correlation and Effective Interionic Potential in a One-Dimensional Ionic Conductor

H. U. Beyeler, L. Pietronero, S. Strässler, and H. J. Wiesmann

Brown Boveri Research Center, CH-5405 Baden, Switzerland

(Received 14 March 1977)

A new method that includes long-range interactions is described and used to compute the site-occupancy correlation in a one-dimensional ionic conductor. The method is applied to hollandite, for which the ions move within independent channels. Through this analysis, we deduce specific information about the interionic potential from experimental data on cationic order. Because of the peculiar screening provided by this material, the potential between mobile ions decays quickly for the first few lattice sites and has only a weak Coulomb tail.

One dimensionality often plays a special role in physical systems. This is the case for ions moving within channels and occupying a fraction ρ of the available sites. The self-diffusion coefficient is zero (for an infinite system) but not the dc conductivity. Furthermore, in one dimension the correlation is very sensitive to details of the

interionic potential.¹

In this Letter, we investigate the general relationship between long-range interionic potentials and the site-occupancy correlation and show to what extent information about the effective interionic potential may be extracted from experimental data about the state of order. As an ap-